Optical Materials 36 (2013) 372–375

Contents lists available at ScienceDirect

Optical Materials

journal homepage: www.elsevier.com/locate/optmat

# Fabrication and characterization of single mode annealed proton exchanged waveguides in -x-cut lithium niobate

O. Yavuzcetin [a,b,*], Nicholas R. Perry [b], Sean T. Malley [b], Rebecca L. Dally [b], Herman P. Novikov [b], Birol Ozturk [b], Srinivas Sridhar [b]

[a] Department of Physics, University of Wisconsin-Whitewater, 800 W. Main St., Whitewater, WI 53190, USA
[b] Electronic Materials Research Institute and Department of Physics, Northeastern University, Boston, MA 02115, USA

ARTICLE INFO

*Article history:*
Received 1 February 2013
Received in revised form 17 September 2013
Accepted 25 September 2013
Available online 25 October 2013

*Keywords:*
Photonics
Waveguide
Lithium niobate
Proton exchange
Optical transmission
Fiber optics

ABSTRACT

Lithium niobate is a key, well-known material in optical communication that maintains its importance due to its high speed in electro-optical modulators and other optical devices. Using a benzoic acid proton exchange method and annealing in wet $O_2$, we have fabricated waveguides along the *y*-axis of -x-cut lithium niobate substrate. We have optimized proton exchange and annealing time to make waveguides with the highest transmission we observed to date. The optical transmission was measured in waveguides between 3 μm and 7 μm in width, and 10 mm in length. The near-field mode properties of the waveguides were also examined. In addition, we discovered that the transmission through waveguides is reduced by the surface residues which are underestimated in most fabrication processes. This paper outlines the full fabrication process as well as characterization methods in detail, including a supercontinuum laser source.

© 2013 Elsevier B.V. All rights reserved.

## 1. Introduction

Lithium Niobate (LN) is commonly used in a variety of applications, including guided-wave optics. Various waveguide manufacturing methods using LN have been established in the past; however, since it is still one of the fastest electro-optical materials in use, research is ongoing and new discoveries are being made [1–3].

LN is transparent for wavelengths ranging from 350 nm to approximately 5 μm, and exhibits a high electro-optic coefficient as well as extraordinary changes in its index of refraction when exposed to a proton exchange process [4,5]. This makes for exceptional optical mode confinement in low loss proton exchanged LN waveguides. One application of these waveguides is to overlay photonic crystals on top for guided light transmission in devices such as sensors. Functional LN photonic crystal devices have yet to be demonstrated, although advancements in the field are still being made [6–8].

Proton exchanged LN waveguides also exhibit a much higher resistance to optical damage than conventional titanium indiffused LN waveguides, making them useful over a broader spectrum of light [9,10]. In this paper, we demonstrate a method for fabricating annealed proton exchanged (APE) waveguides in -x-cut LN. We discuss our experimentation with duration of both a benzoic acid proton exchange process and wet $O_2$ annealing, as well as an outline of optical characterization methods and results for the fabricated waveguides. We find that, surface cleaning has a key role in the transmission of light through waveguides.

## 2. Procedure

### 2.1. APE process

We have developed a process to create waveguides in -x-cut LN wafers (Crystal Technology Inc.). The steps of this process are as follows: the deposition of titanium and photoresist masks on the LN substrate, photolithography and wet etching to create the waveguide pattern, and proton exchange and annealing processes (see Fig. 1).

First, the wafers were cleaned via sonication in acetone, followed by isopropanol, and then blow dried with nitrogen. A 150 nm thick titanium mask layer was deposited on the wafers using an e-beam evaporator (Denton). The depth was measured

* Corresponding author at: Department of Physics, University of Wisconsin-Whitewater, 800 W. Main St., Whitewater, WI 53190, USA. Tel.: +1 206 472 1076.
*E-mail addresses:* yavuzceo@uww.edu (O. Yavuzcetin), perry.n@husky.neu.edu (N.R. Perry), malley.s@husky.neu.edu (S.T. Malley), dallyr@bc.edu (R.L. Dally), HermanNovikov2013@u.northwestern.edu (H.P. Novikov), birolozturk@gmail.com (B. Ozturk), s.sridhar@neu.edu (S. Sridhar).

0925-3467/$ - see front matter © 2013 Elsevier B.V. All rights reserved.
http://dx.doi.org/10.1016/j.optmat.2013.09.025

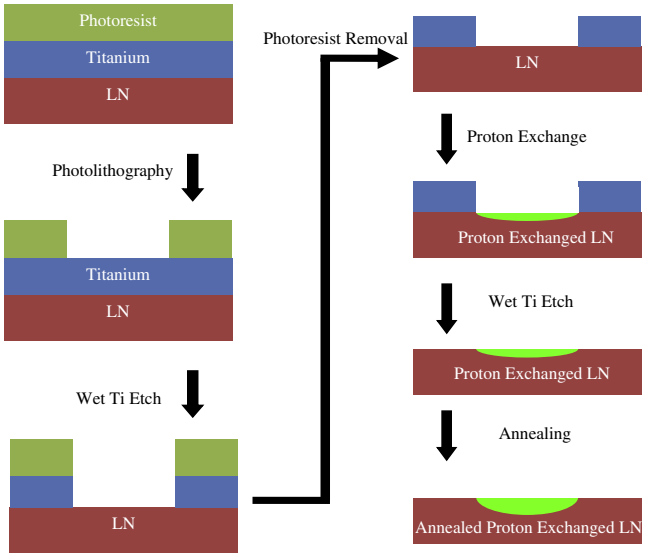


**Fig. 1.** Process flow for creating APE waveguides: waveguide pattern transfer to LN through photoresist and titanium masks by photolithography and wet etching, proton exchange, mask removal, and annealing steps.

using a profilometer (Dektak 3ST). Microposit® S1813 photoresist (Shipley) was spin-coated on the titanium in two steps. The first step lasted 8 s at 500 rpm with an acceleration of 110 rpm/s, followed by 4000 rpm for 1 min at an acceleration of 1650 rpm/s. The wafers were pre-baked at 115 °C for 1 min and exposed to UV light by photolithography (Quintel 4000) for 8 s. The LN wafers were aligned such that the waveguides ran parallel with the *y*-axis. This orientation was chosen because the electro-optic coefficient ($r_{33}$) is the highest in the z-direction [11]. The waveguide widths on the photomask were 3, 4, 5, 6, and 7 μm. The development was done by rinsing the wafers in Microposit® MF®-319 developer (Shipley) for 35 s, then rinsing in de-ionized (DI) water, and then drying with a nitrogen gun. The wafer was post-baked at 115 °C for 2 min. The exposed titanium was wet etched, with the photoresist serving as a mask. The titanium etch recipe was 5:1:1 of DI water, $H_2O_2$ (29%), and $NH_4OH$ (30%), respectively by volume. The etch rate of a fresh solution is about 0.4 nm/s, but its reactivity, and therefore etch rate, is dependent on its age. If the etch rate decreases, some hydrogen peroxide can be added as a catalyst to speed up the reaction. The wafers were rinsed in DI water and nitrogen dried. 1813 photoresist was removed in Microposit® Remover 1165 (Shipley) at 65 °C for 10 min.

To prevent damage due to debris during dicing, a protective coating was applied to the sample using Microposit® S1827 (Shipley). It was spin-coated on the wafer at 3000 rpm for 1 min to yield a layer about three microns thick. The wafer was baked at 115 °C for 30 s. The wafers were diced into small rectangular pieces (10 mm × 12 mm) using a dicing saw, and the 1827 photoresist was removed.

Proton exchange between the $Li^+$ and $H^+$ ions was performed using pure benzoic acid (BA). The sample and BA were placed in a double neck flask with Teflon® coated thermocouple and a temperature probe, seated on a heating mantle. The setup employs a temperature controlled water jacket distilling column. The BA was heated to 220 °C, and the sample remained in the flask for times ranging from one to three hours [12]. Once the samples were removed from the BA, they were sonicated in dimethylsulfoxide (DMSO) and isopropanol for 2 min each.

The areas exposed to the proton exchange exhibited an increased index of refraction, supported by previous studies [13,14]. The remaining titanium was removed from the samples using the same titanium etch recipe from earlier in the process. We observed that the titanium etch took significantly longer (~30 min) after the proton exchange process. This may be due to changes in the surface of titanium during the proton exchange process.

The samples were annealed in a tube furnace under water vapor flow in order to diffuse the exposed areas with the changed index of refraction further into the LN (Fig. 1) [15,16]. The water vapor was produced by sending $O_2$ at a rate of 10 mL/min through a flask of water heated to 85 °C. [17]. The furnace temperature was increased at a rate of 2 °C/min and the temperature was held at 400 °C for 3 h. Following the 3 h bake, the $O_2$ flow rate was reduced to 5 mL/min and the furnace temperature was brought down at a rate of 1 °C/min, settling at room temperature [18]. One sample was reserved for SEM imaging, while others were prepared for polishing and optical characterization. Fig. 2 shows scanning electron microscope (SEM) images of a gold sputtered 3 μm wide waveguide created in the LN sample.

If either the $O_2$ flow rate or water temperature were too high during the annealing process, cracking in the LN was observed. Increasing the rate of temperature change inside the annealing furnace also caused the LN to crack.

The titanium mask also proved resistant to wet etching if it remained on the sample during annealing. Because of this, titanium was removed from the samples following the proton exchange process and prior to annealing.

### 2.2. Polishing

Following the APE process and prior to optical testing, edge polishing of the samples was required to reduce coupling losses. The edges of the diced samples were polished in a four step process. Before polishing, the sample was mounted on an angled aluminum block with a thermal polymer (Crystalbond 509). This mount enabled the input and output edges of the sample to be polished at a 6° angle (Fig. 3), which reduces reflections in optical testing. The sample and block were then placed in a cross section fixture (Accelerated Analysis PF101).

Next, the sample was hand polished on a 600 μm grit silicon carbide polishing pad. Polishing the sample in a motion uniformly grinds down the edge of the sample to eliminate any damage done from dicing. The next two steps use a 9 μm diamond lapping film, followed by a 3 μm film. The final polishing step uses a colloidal silica polishing compound on a Chemomet® (Beuhler) polishing pad.

Once polished, the samples were removed from the aluminum blocks and cleaned with acetone in an ultrasonic bath for 3 min, then rinsed with isopropanol and dried with compressed air. Thorough cleaning of the sample is essential to achieve coupling into the waveguide. No transmission was observed in samples with visible residue on the surface, but following proper cleaning, transmission was apparent.

### 2.3. Optical characterization

Optical characterization was performed to evaluate mode-field distribution and waveguide losses following APE, polishing, and cleaning. Fig. 4a depicts the layout of the optical alignment setup. When imaging in the near-field mode, a tunable SANTEC diode laser (TSL-210H) was employed as the source which was set to a 1550 nm wavelength. As the laser source was unpolarized, its output was coupled to a polarization scrambler (FIBERPRO PS-155-A-B) and passed through an in-line fiber polarizer. This TE polarized source was coupled to a polarization maintaining (PM) fiber. The end facet of this PM fiber was 8° angle polished and butt coupled to the LN APE waveguide. The alignment was done by mounting

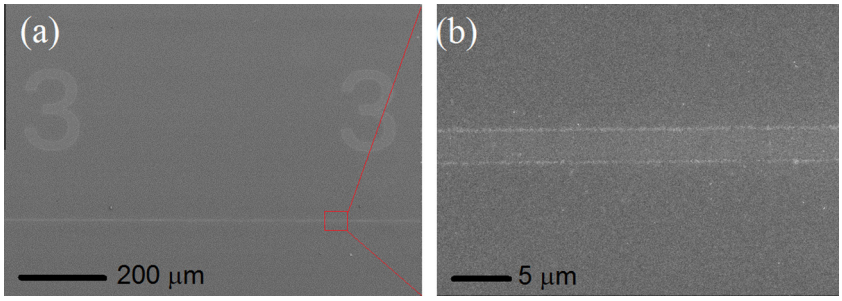


**Fig. 2.** (a) An SEM image of 3 μm wide APE waveguide in LN, and its label. The scale bar denotes 200 μm (b) A higher magnification SEM image of the same 3 μm wide waveguide. The scale bar denotes 5 μm.


**Fig. 3.** Angle polished LN sample and crystal axis orientation.

the input fiber on a 6-axis stage (Thorlabs MAX603) where the sample was placed on a stationary stage. The transmitted output was collected at the end facet of the waveguides with a 20X objective lens mounted on a second 6-axis stage and the near-field mode image was captured with an IR camera (Hamamatsu C2741). The near-field mode image of a 5 μm wide waveguide displayed single-mode characteristics at 1550 nm (Fig. 4b). In order to measure the transmission loss, the objective lens at the output facet was replaced with another angled PM fiber which was coupled to an InGaAs photodetector. (Thorlabs DET01CFC). The optical transmission loss of the 5 μm wide APE waveguides was as low as 10 dB/cm at 1550 nm.

A supercontinuum laser (SuperK Versa) was used as the source in order to determine the broadband optical transmission spectrums of the waveguides (Fig. 5a).

The output of the supercontinuum laser was split into visible and IR using the SpectraK Split (NKT Photonics) accessory where the IR output was polarized with a nanoparticle linear film polarizer (Thorlabs LPNIR). This IR output was coupled to a polarization

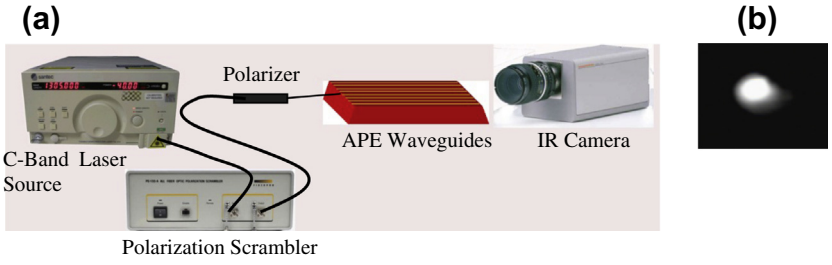


**Fig. 4.** (a) Optical setup for fiber-waveguide alignment. (b) Near-field mode image of a 5-μm wide waveguide at 1550 nm.

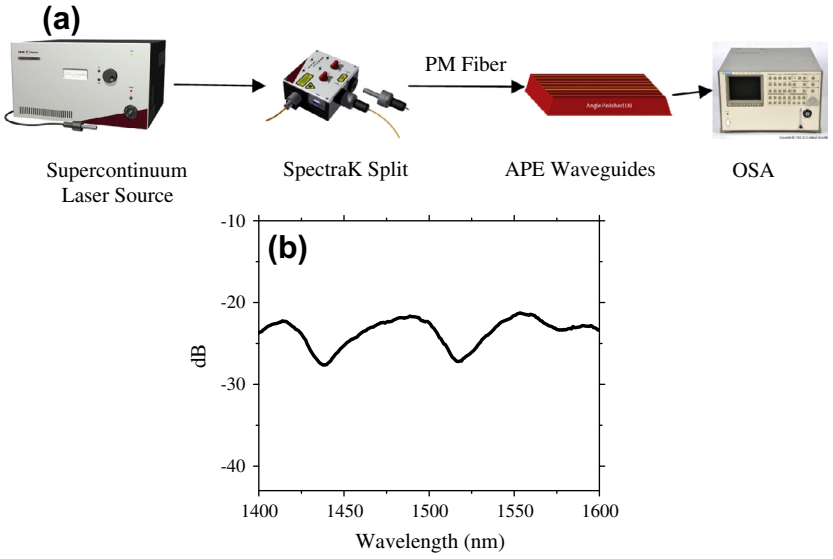


**Fig. 5.** (a) Optical characterization test setup. After travelling through waveguides, light can either be collected by an IR camera or run to an OSA via a PM fiber. (b) Optical transmission spectrum of a 5 μm wide waveguide in the 1400–1600 nm range.

maintaining (PM) optical fiber, introducing the linearly polarized (TE) source to the input of the waveguide. The output was recorded with an optical spectrum analyzer (OSA) (Ando AQ-6310B). Fig. 5b shows the optical transmission spectrum of the 5 micron wide APE waveguide in the 1400–1600 nm range. The waveguide displayed wavelength dependent intensity profile in the transmission spectrum.

## 3. Conclusion

Using a benzoic acid proton exchange and wet $O_2$ annealing process, APE waveguides were successfully created in LN substrates. The waveguides ranged in width from 3 to 7 μm and exhibited single mode transmission.

The waveguides demonstrated acceptable losses, the best being a 10 dB/cm insertion loss in a 5 μm waveguide at 1550 nm.

With photonic crystal structures overlaid on the surface of these waveguides, there is potential for low perturbation electric field sensing. Coupled to a side polished optical fiber, such electric field sensors can be used in monitoring the electrical activity in the human body or in sensitive electrical components. Most electric field sensors in use today are comprised of metal components which significantly affect the fields they are trying to monitor. An all dielectric photonic crystal sensor would greatly mitigate the disturbance to the electric fields in question caused by a conventional sensor's metallic components, leading to more accurate measurements of electric field properties.

## Acknowledgements

This work was performed in part at the Center for Nanoscale Systems (CNS), a member of the National Nanotechnology Infrastructure Network (NNIN), which is supported by the National Science Foundation under NSF Award No. ECS-0335765. CNS is part of Harvard University. Research was carried out in part at the Center for Functional Nanomaterials, Brookhaven National Laboratory, which is supported by the U.S. Department of Energy, Office of Basic Energy Sciences, under Contract No. DE-AC02-98CH10886. Research was carried out in part at the Electronic Materials Research Institute at Northeastern University, the Kostas Nanoscale Technology. The experimental results were in part analyzed at the University of Wisconsin-Whitewater.

This research was sponsored by the Defense Advanced Research Projects Agency, Electric Field Detector (E-FED) Program, issued by DARPA/CMO under Contract No. HR0011-10-C-0043. The views expressed are those of the authors and do not reflect the official policy or position of the Department of Defense or the U.S. Government. DISTRIBUTION STATEMENT A. Approved for public release; distribution is unlimited.

## References

[1] M.L. Bortz, M.M. Fejer, Annealed proton-exchanged $LiNbO_3$ waveguides, Opt. Lett. 16 (1991) 1844–1846.
[2] H. Hu, R. Ricken, W. Sohler, R.B. Wehrspohn, Lithium niobate Ridge waveguides fabricated by wet etching, IEEE Photon. Tech. Lett. 19 (6) (2007) 417–419.
[3] C.J.G. Kirkby, C. Florea, Dispersion properties of LiNbO and tables, in: K.K. Wong (Ed.), Properties of Lithium Niobate, INSPEC, 2002, pp. 119–128.
[4] H. Hui, R. Ricken, W. Sohler, Etching of lithium niobate: from Ridge waveguides to photonic crystal structures, Angew. Phys., Univ. Paderborn (2008).
[5] L. Arizmendi, Photonic applications of lithium niobate crystals, Phys. Status Solidi 201 (2004) 253–283.
[6] O. Yavuzcetin, H.P. Novikov, R.L. Dally, S.T. Malley, N.R. Perry, B. Ozturk, S. Sridhar, Photonic crystal fabrication in lithium niobate via pattern transfer through wet and dry etched chromium mask, J. Appl. Phys. 112 (2012) 074303.
[7] O. Yavuzcetin, B. Ozturk, D. Xiao, S. Sridhar, Conicity and depth effects on the optical transmission of lithium niobate photonic crystals patterned by focused ion beam, Opt. Mater. Express 1 (2011) 1262–1271.
[8] H. Hartung, E.B. Kley, T. Gischkat, F. Schrempel, W. Wesch, A. Tunnermann, Ultra thin high index contrast photonic crystal slabs in lithium niobate, Opt. Mater. 33 (2010) 19–21.
[9] P. Rabiei, P. Gunter, Optical and electro-optical properties of submicrometer lithium niobate slab waveguides prepared by crystal ion slicing and wafer bonding, Appl. Phys. Lett. 85 (2004) 4603–4605.
[10] G.R. Paz-Pujalt, D.D. Tuschel, G. Braunstein, T. Blanton, S.T. Lee, L.M. Salter, Characterization of proton exchange lithium niobate waveguides, J. Appl. Phys. 76 (1994) 3981–3987.
[11] R.S. Weis, T.K. Gaylord, Lithium niobate: summary of physical properties and crystal structure, Appl. Phys. A: Mater. Sci. Proc. 37 (1985) 191–203.
[12] P. Nekvindova, J. Spirkova, J. Cervena, M. Budnar, A. Razpet, B. Zorko, P. Pelicon, Annealed proton exchanged optical waveguides in lithium niobate: differences between the X- and Z-cuts, Opt. Mater. 19 (2002) 245–253.
[13] M. Bernal, N. Courjal, J. Amet, M. Roussey, C.H. Hou, Lithium niobate photonic crystal waveguides: far field and near field characterization, Opt. Commun. 265 (2006) 180–186.
[14] A. Loni, R.W. Keys, R.M. De La Rue, M.A. Foad, J.M. Winfield, Optical characterization of Z-cut proton-exchanged $LiNbO_3$ waveguides fabricated using orthophosphoric and pyrophosphoric acid, IEEE Proc. J. 136 (1989) 297–300.
[15] V. Bermúdez, D. Callejo, E. Diéguez, Effect of temperature annealing on periodically poled rare-earth doped lithium niobate crystal, J. Optoelectron. Adv. M 5 (2003) 55–59.
[16] J. Rams, J.M. Cabrera, Preparation of proton-exchange $LiNbO_3$ waveguides in benzoic acid vapor, JOSA B 16 (1999) 401–406.
[17] D.C. Cromer, G.N. De Brabander, J.T. Boyd, H.E. Jackson, S. Sriram, Use of a rapid thermal annealing system to initiate indiffusion for fabrication of Ti:$LiNbO_3$ optical channel waveguides, Appl. Opt. 28 (1989) 33–36.
[18] L. Burrows, Method for pressurized annealing of lithium niobate and resulting lithium niobate structures, US Patent 6,770,132 B1, (1999).